

Analysis of the Spatial Errors of the Scanning Mirrors in Complex Optical and Mechanical Systems

Dongxu Jiang¹, Yingchun Li¹, Minghui Gao², Baoyu Sun¹, Jieqiong Lin^{1,*}

¹School of Mechatronic Engineering, Changchun University of Technology, Changchun 130000, China.

²Changchun Institute of Optics, Fine Mechanics and Physics, Chinese Academy of Science, Changchun 130000, China.

*Corresponding author e-mail: linjieqiong@ccut.edu.cn

Abstract. In recent years, in order to improve the imaging performance of complex optical and mechanical components in complex working environments, scanning mirrors are used as main optical components that precisely control the direction of beam propagation. They can not only expand the range of photography, but also suppress the shift error caused by attitude changes. So scanning mirrors are widely used in the fields of aerial cameras, satellite remote sensing and military investigation. In the process of machining and assembling the scanning mirror platform, pointing error will be produced which directly affects the imaging quality of the camera which acquires the ground image by the reflection of the scanning mirrors. Taking the two-axis scanning mirror as an example, the global error model is established based on the homogeneous coordinate transformation theory. The simulation analysis is carried out to compare the influence of each error to the pointing error of the scanning mirror. In the process of designing and processing scanning mirror, the error items which have great influence to the pointing error of the scanning mirror should be strictly controlled or taken some corresponding measures. It is very important to improve the pointing accuracy of scanning mirror to enhance the imaging quality of the aerial camera.

Keywords: optical and mechanical system; scanning mirror; pointing error; geometric error.

1. Introduction

Complex optical and mechanical system (such as aerial camera) is one of the most important means to obtain ground information. Image motion errors generated by the change of the attitudes (roll and pitch) of the aircraft can be compensated through using scanning mirror in the process of flying. Scanning mirror can also realize the optical path folding and reasonable layout of the camera. Therefore, the performance of the scanning mirror directly affects the imaging quality of the aerial camera [1]. In order to keep the optical axis reflected by the scanning mirror stable, mirror pitch axis and azimuth axis system perform corresponding angular motions to compensate the change of attitude of the aircraft. Pointing error is used to characterize performance of the optical path folding. Image quality is an important performance indicator of complex optical and mechanical systems (such as aerial cameras) [2]. When



the aircraft is flying in the air, the imaging quality is affected by many factors which includes environment, hardware conditions and carrier platforms.

The geometric error of the scanning mirror will be studied in this paper. Since the complex optical and mechanical system (such as aerial camera) acquires image on the ground by the reflection of the scanning mirror, the frames of the scanning mirror and the shafting are scanned. The accuracy between the structure and the entire size chain will directly affect the quality of the aerial camera's acquisition of ground images. Geometric errors such as mounting error between frames, mounting errors between shafting and transmission errors are the main error sources of the mirror pointing errors.

2. Geometric error analysis of scanning mirror in complex optical and mechanical system

2.1. The structure composition of the scanning mirror in complex optical and mechanical system

Based on the kinematics principle [3], any rotating motion of the scanning mirror in inertial space can be decomposed into angular motions of three vertical axial. The typical two-axis scanning mirror is shown in figure 1. It is composed of azimuth axis and pitch axis from outside to inside which are connected with angular displacement sensors. The scanning mirror is mounted on the aircraft through the base. The scanning mirror is rigidly connected to the platform base. The base is connected with the azimuth frame (outer frame) through the azimuth shafting. The azimuth frame is connected with the pitching frame (inner frame) by the pitching shafting. The scanning mirror is directly fixed in the pitch frame through the assembling ring.

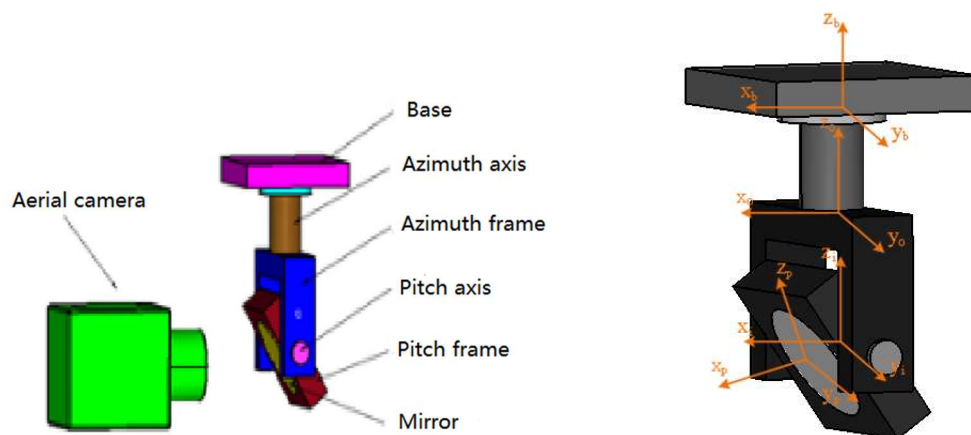


Fig. 1 Two-axis azimuth-pitch scanning mirror platform. **Fig. 2** Coordinate system of scanning mirror.

2.2. Analysis of geometric error sources of scanning mirror in complex optical and mechanical system

Geometric errors will be generated for the actual position of each component deviated from its ideal position in the manufacturing and assembling scanning mirrors [3]. Based on the error modeling theory of multi-body system, the position error will be produced when any two adjacent bodies are connected, the motion error will be produced by the relative motion [4]. The geometric error sources which affect the pointing error mainly include the vertical errors of the shafting, the rotation errors of the shafting and the transmission errors of the shafting [5]. The vertical errors of shafting belong to position errors and the rotation errors and the transmission errors of the shafting belong to motion errors. The coordinate systems of scanning mirrors are set up in Figure 2 to express the geometric errors.

The stability of the optical path can be maintained through two-axe azimuth and pitch scanning mirror. For the pointing error will not be affected by the intersection errors of the shafting system, the axial movement errors and the radial eccentricity errors, which are neglected in this paper. The physical meanings and expressions of the geometric errors are shown in Table 1.

Table 1. The error sources of the two-axe azimuth and pitch scanning mirror.

coordinate system	position error	representation	coordinate system	motion error	representation
{b} system	vertical error of azimuth axis relative to the base(rotated around y_b axis)	δ_{oby}	{o} system	rotation error of the azimuth axis(rotated around y_o axis)	$\Delta\gamma_{oy}$
				rotation error of the azimuth axis(rotated around x_o axis)	$\Delta\gamma_{ox}$
{o} system	vertical error of pitch axis relative to azimuth axis(rotated around x_o axis)	δ_{iox}	{i} system	rotation error of the pitch shaft(rotated around x_i axis)	$\Delta\gamma_{ix}$
				rotation error of the pitch shaft(rotated around z_i axis)	$\Delta\gamma_{iz}$
{i} system	vertical error of the pointing axis relative to the pitch axis(rotated around z_i axis)	δ_{piz}	{o} system	transmission error of the azimuth shaft(rotated around z_o axis)	$\Delta\theta_{oz}$
			{i} system	transmission error of the pitching shaft(rotated around y_i axis)	$\Delta\theta_{iy}$

3. Error model establishment of scanning mirror in complex optical and mechanical system

Based on the definition of the coordinate system, the direction vector in the base coordinate system is converted to the mirror pointing coordinate system. In the base coordinate system, the mirror unit

direction vector is defined as $\vec{r}_p = \left[\frac{\sqrt{2}}{2}, 0, -\frac{\sqrt{2}}{2} \right]$. Ideally, the unit vector in the mirror pointing

coordinate system is \vec{r}_i . In actually, there exist errors in the complex optical and mechanical systems.

The unit vector in the mirror pointing coordinate system is \vec{r}_p . Based on the homogeneous coordinate transformation theory, the relative coordinate transformation relationship between the inner frame and the base is obtained by using the coordinate transformation matrix. In this paper, the rotation coordinate transformation matrix is written in $rot(v, \theta)$ in the formula (2), which is rotated θ angle relative to the original coordinate system v axis (v, x, y, z). The direction of the visual axis will not be affected by the translation of the coordinate system, so the translation of the origin of coordinate system is not considered in the coordinate transformation matrix.

Ideally, \vec{r}_i can be obtained through the coordinate transformation of the scanning mirror which is shown in formula (1).

$$\begin{aligned}
 \vec{r}_i &= T_{bo} T_{oi} \vec{r}_p \\
 &= rot(z_o, \alpha) rot(y_i, \beta) \vec{r}_p \\
 &= \begin{bmatrix} \cos\alpha & -\sin\alpha & 0 \\ \sin\alpha & \cos\alpha & 0 \\ 0 & 0 & 1 \end{bmatrix} \begin{bmatrix} \cos\beta & 0 & \sin\beta \\ 0 & 1 & 0 \\ -\sin\beta & 0 & \cos\beta \end{bmatrix} \begin{bmatrix} \frac{\sqrt{2}}{2} \\ 0 \\ -\frac{\sqrt{2}}{2} \end{bmatrix} \tag{1}
 \end{aligned}$$

In this paper, the actual direction vector of the reflector is deduced considering the verticality error, shaft rotation error and shafting transmission error.

(1) The transformation matrix is considered the transformation error between the base coordinate system and the azimuth coordinate system [6-7]. The errors between the base coordinate system and the azimuth coordinate system mainly include the perpendicularity error δ_{oby} of the azimuth axis relative to the base, azimuth shaft transmission error $\Delta\theta_{bz}$, azimuth axis rotation error $\Delta\gamma_{oy}$, $\Delta\gamma_{ox}$. Based on the kinematical theory, the matrix transformation relation between two coordinate systems can be obtained as shown in formula (2).

$$\begin{aligned}
 T_{bo}^a &= rot(y_b, \delta_{oby})rot(z_o, \alpha + \Delta\theta_{bz})rot(y_o, \Delta\gamma_{oy})rot(x_o, \Delta\gamma_{ox}) \\
 &= \begin{bmatrix} \cos\delta_{oby} & 0 & \sin\delta_{oby} \\ 0 & 1 & 0 \\ -\sin\delta_{oby} & 0 & \cos\delta_{oby} \end{bmatrix} \times \begin{bmatrix} \cos(\alpha + \Delta\theta_{bz}) & -\sin(\alpha + \Delta\theta_{bz}) & 0 \\ \sin(\alpha + \Delta\theta_{bz}) & \cos(\alpha + \Delta\theta_{bz}) & 0 \\ 0 & 0 & 1 \end{bmatrix} \times \begin{bmatrix} \cos\Delta\gamma_{oy} & 0 & \sin\Delta\gamma_{oy} \\ 0 & 1 & 0 \\ -\sin\Delta\gamma_{oy} & 0 & \cos\Delta\gamma_{oy} \end{bmatrix} \\
 &\times \begin{bmatrix} 1 & 0 & 0 \\ 0 & \cos\Delta\gamma_{ox} & -\sin\Delta\gamma_{ox} \\ 0 & \sin\Delta\gamma_{ox} & \cos\Delta\gamma_{ox} \end{bmatrix}
 \end{aligned} \tag{2}$$

(2) The error transformation matrix is shown in formula (3) which is between the azimuth coordinate system of the reflector and the pitch coordinate system.

$$\begin{aligned}
 T_{oi}^a &= rot(x_o, \delta_{iox})rot(y_i, \beta + \Delta\theta_{iy})rot(x_i, \Delta\gamma_{ix})rot(z_i, \Delta\gamma_{iz}) \\
 &= \begin{bmatrix} 1 & 0 & 0 \\ 0 & \cos\delta_{iox} & -\sin\delta_{iox} \\ 0 & \sin\delta_{iox} & \cos\delta_{iox} \end{bmatrix} \times \begin{bmatrix} \cos(\beta + \Delta\theta_{iy}) & 0 & \sin(\beta + \Delta\theta_{iy}) \\ 0 & 1 & 0 \\ -\sin(\beta + \Delta\theta_{iy}) & 0 & \cos(\beta + \Delta\theta_{iy}) \end{bmatrix} \times \begin{bmatrix} 1 & 0 & 0 \\ 0 & \cos\Delta\gamma_{ix} & -\sin\Delta\gamma_{ix} \\ 0 & \sin\Delta\gamma_{ix} & \cos\Delta\gamma_{ix} \end{bmatrix} \\
 &\times \begin{bmatrix} \cos\Delta\gamma_{iz} & -\sin\Delta\gamma_{iz} & 0 \\ \sin\Delta\gamma_{iz} & \cos\Delta\gamma_{iz} & 0 \\ 0 & 0 & 1 \end{bmatrix}
 \end{aligned} \tag{3}$$

(3) The error transformation matrix is shown in formula (4) which is between the mirror coordinate system and the pitching coordinate system.

$$\begin{aligned}
 T_{ip}^a &= rot(z_i, \delta_{piz}) \\
 &= \begin{bmatrix} \cos\delta_{piz} & -\sin\delta_{piz} & 0 \\ \sin\delta_{piz} & \cos\delta_{piz} & 0 \\ 0 & 0 & 1 \end{bmatrix}
 \end{aligned} \tag{4}$$

The actual direction vector \vec{r}^a in the pointing coordinate system can be gotten from the transformation matrixes considering the errors between the above coordinate systems, which is shown in formula (5).

$$\begin{aligned}
 \vec{r}_a &= T_{bo}^a T_{oi}^a T_{ip}^a \vec{r}_b \\
 &= \begin{bmatrix} \cos\delta_{by} & 0 & \sin\delta_{by} \\ 0 & 1 & 0 \\ -\sin\delta_{by} & 0 & \cos\delta_{by} \end{bmatrix} \times \begin{bmatrix} \cos(\alpha + \Delta\theta_z) & -\sin(\alpha + \Delta\theta_z) & 0 \\ \sin(\alpha + \Delta\theta_z) & \cos(\alpha + \Delta\theta_z) & 0 \\ 0 & 0 & 1 \end{bmatrix} \times \begin{bmatrix} \cos\Delta\gamma_{oy} & 0 & \sin\Delta\gamma_{oy} \\ 0 & 1 & 0 \\ -\sin\Delta\gamma_{oy} & 0 & \cos\Delta\gamma_{oy} \end{bmatrix} \\
 &\times \begin{bmatrix} 1 & 0 & 0 \\ 0 & \cos\Delta\gamma_{ox} & -\sin\Delta\gamma_{ox} \\ 0 & \sin\Delta\gamma_{ox} & \cos\Delta\gamma_{ox} \end{bmatrix} \times \begin{bmatrix} 1 & 0 & 0 \\ 0 & \cos\delta_{ox} & -\sin\delta_{ox} \\ 0 & \sin\delta_{ox} & \cos\delta_{ox} \end{bmatrix} \times \begin{bmatrix} \cos(\beta + \Delta\theta_y) & 0 & \sin(\beta + \Delta\theta_y) \\ 0 & 1 & 0 \\ -\sin(\beta + \Delta\theta_y) & 0 & \cos(\beta + \Delta\theta_y) \end{bmatrix} \quad (5) \\
 &\times \begin{bmatrix} 1 & 0 & 0 \\ 0 & \cos\Delta\gamma_{ix} & -\sin\Delta\gamma_{ix} \\ 0 & \sin\Delta\gamma_{ix} & \cos\Delta\gamma_{ix} \end{bmatrix} \times \begin{bmatrix} \cos\Delta\gamma_{iz} & -\sin\Delta\gamma_{iz} & 0 \\ \sin\Delta\gamma_{iz} & \cos\Delta\gamma_{iz} & 0 \\ 0 & 0 & 1 \end{bmatrix} \times \begin{bmatrix} \cos\delta_{piz} & -\sin\delta_{piz} & 0 \\ \sin\delta_{piz} & \cos\delta_{piz} & 0 \\ 0 & 0 & 1 \end{bmatrix} \times \begin{bmatrix} \frac{\sqrt{2}}{2} \\ 0 \\ -\frac{\sqrt{2}}{2} \end{bmatrix}
 \end{aligned}$$

The pointing error of the scanning mirror is shown in formula (6).

$$\Delta\varphi = \arccos \left(\frac{\vec{r}_a \cdot \vec{r}_i}{|\vec{r}_a| |\vec{r}_i|} \right) \quad (6)$$

4. Error analysis of the scanning mirror in complex optical and mechanical system

The sensitivity of the errors of the scanning mirror is analyzed supposing that each error acts alone to obtain the effect of each error to the pointing error. In this paper, the rotation range (α) of azimuth axis of the scanning mirror is set as $\pm 0.125 \pi$, rotation range (β) of pitch axis of the scanning mirror is set as $\pm 0.25 \pi$. Fig. (3-7) show the effects of the geometric errors to the pointing errors.

4.1. Influence of shafting verticality error to the pointing error

As shown in Fig. 3, the minimum value of the pointing error is 9.6×10^{-4} rad which is caused by the perpendicularity error δ_{oby} between the azimuth axis and the pedestal, the maximum value is 1×10^{-3} rad, the range of variation is 4×10^{-5} rad, the mean value is 9.9635×10^{-4} rad and the mean square value is 5.7156×10^{-6} rad.

As shown in Fig. 4, the minimum error value of the pointing error is 2.5×10^{-4} rad which is caused by the vertical error δ_{iox} between the pitch axis and the azimuth axis, the maximum value is 1×10^{-3} rad, the range of variation is about 7.5×10^{-4} rad, the mean value is 7.9247×10^{-4} rad and the root mean square value is 2.1664×10^{-4} rad.

As shown in Fig. 5, the minimum value of the pointing error is 4×10^{-4} rad which is caused by the verticality error δ_{piz} between the vertical axis and pitch axis, the maximum value of 4.5×10^{-4} rad, the range of the variation is 5×10^{-5} rad, the mean value is 4.4084×10^{-4} rad and the root mean square value 9.9723×10^{-6} rad.

The perpendicularity error δ_{iox} is the most influential error to the pointing error which is between the pitch axis and the azimuth axis. The other two perpendicularity errors are relatively small.

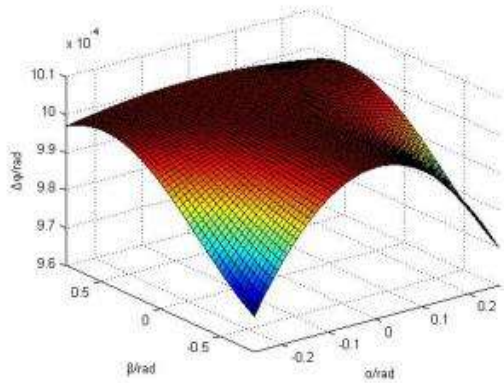


Fig. 3 Influence of $\delta\beta$ to pointing error.

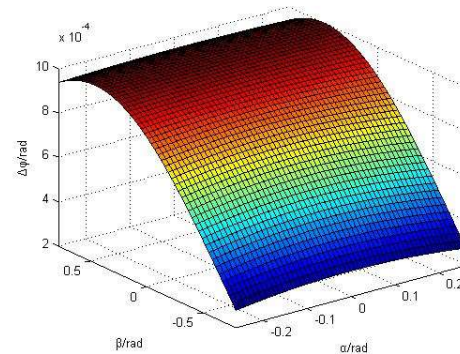


Fig. 4 Influence of $\delta\alpha$ to pointing error.

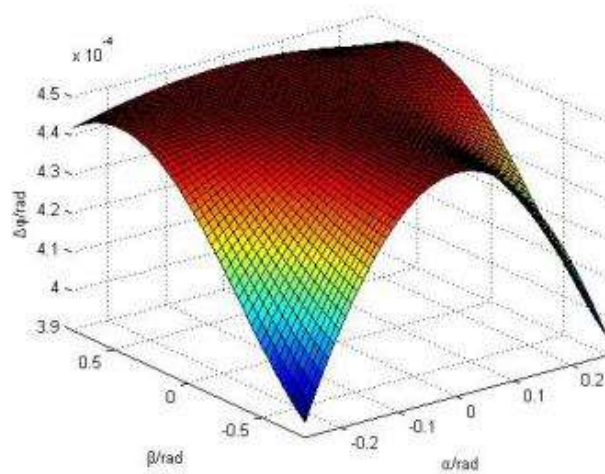


Fig. 5 Influence of $\delta\pi_z$ to the pointing error.

4.2. Influence of the shafting rotation error to the pointing error

As shown in Fig. 6, the azimuth axis rotation error $\Delta\gamma_{ox}$ has the most important influence to the pointing error. The other three error terms have less influence.

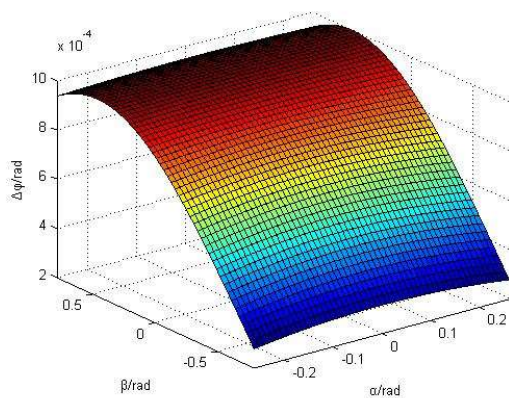


Fig. 6 Influence of $\Delta\gamma_{ox}$ to the pointing error.

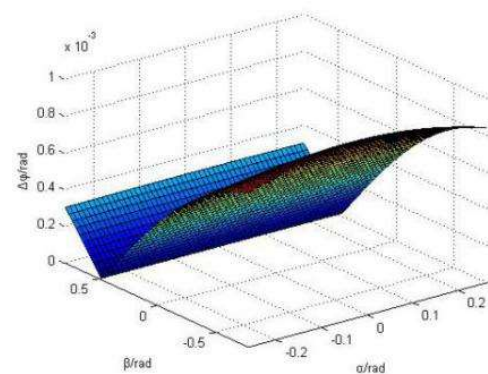


Fig. 7 Influence of $\Delta\theta_{oz}$ to the pointing error.

4.3. Influence of shafting transmission error to the pointing error

The maximum value of the pointing error is 1×10^{-3} rad which is caused by both azimuth axis and pitch axis. But the transmission error $\Delta\theta_{oz}$ of the azimuth axis is larger than that of azimuth axis, which has a greater influence to the pointing error.

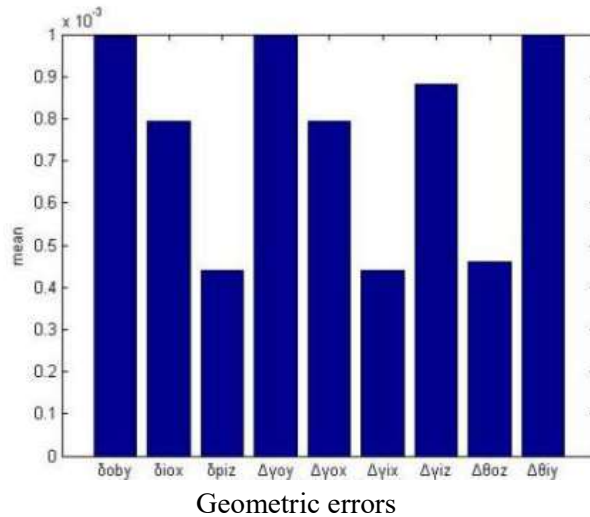


Fig. 8 Mean values of the pointing error caused by geometric errors.

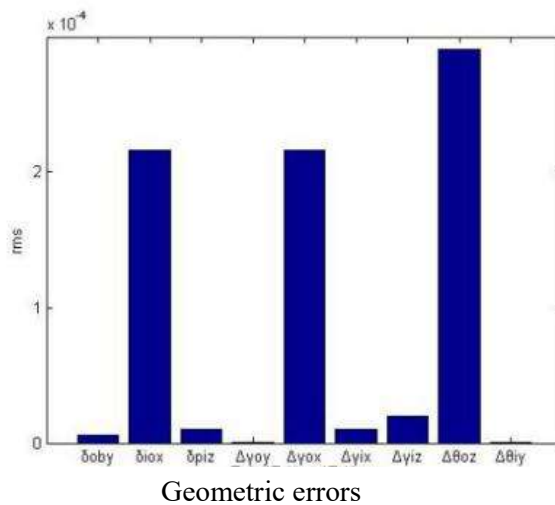


Fig. 9 Mean square values of the pointing error caused by geometric errors.

Fig. 8 and Fig. 9 show the mean values and the mean square values of the pointing error caused by geometric errors, respectively. The errors δ_{ox} , Δ_{gox} and $\Delta\theta_{oz}$ have great influence to the pointing error which can be seen from the figures. The steering error around the x-axis has a greater influence than others. It's necessary to take measures to compensate the greater impact errors to the pointing error of the scanning mirrors.

5. Conclusion

In this paper, the spatial errors of the scanning mirrors in the complex optical and mechanical systems are introduced. An overall error model of the scanning mirror is established through analyzing various error sources. The vertical axis error δ_{ox} , the azimuth axis transmission error $\Delta\theta_{oz}$ and the azimuth

axis rotation error $\Delta\gamma_{ox}$ between the pitch axis and the azimuth axis have greater influence to the pointing error through the analysis results. These errors should be compensated to improve the pointing error of the scanning mirror. This research can provide a theoretical basis for designing and manufacturing the scanning mirrors in the optical and mechanical system.

Acknowledgments

This work was financially supported by China Science and Technology Department (2016YFE0105100), Jilin Science and Technology Office (20180201052GX) and The Education Department of Jilin Province (2016334).

References

- [1] Sun A Y, Wang D, Xu X. Monthly stream flow forecasting using Gaussian process regression[J]. *Journal of Hydrology*, 2014, 511: 72-81.
- [2] Hong H, Zhou X, Zhang Z, et al. Modeling and calibration of pointing errors using a semi-parametric regression method with applications in inertially stabilized platforms [J]. *Proceedings of the Institution of Mechanical Engineers, Part B: Journal of Engineering Manufacture*, 2013, 227(10): 1492-1503.
- [3] Yun Fu, Changji Xu, Yalin Ding. Scanning mirror support technology for aerial remote sensing camera [D], 2003.
- [4] Xiao-yao Zhou. Analysis and Correction of Target Positioning error in photoelectric Detection system [D]. Changsha: University of National Defense Science and Technology, 2011.
- [5] Qijian Tang. Analysis and Research on pointing error of High Precision Multi-axis stabilized platform [D]. Tianjin University, 2014
- [6] Ming Zhao. Error Analysis and compensation of Semi-Strapdown photoelectric stabilized platform [D]. Beijing: University of the Chinese Academy of Sciences, 2014.
- [7] Zhongyu Liu. Research on Error Analysis and Structure Optimization of Semi-Striker Aviation Remote Sensing Platform [D]. Changchun Institute of Optics, Fine Mechanics and Physics, Chinese Academy of Sciences, 2016.